Microbiol. Immunol., 51(7), 661–669, 2007

Characterization of Prion Susceptibility in Neuro2a Mouse Neuroblastoma Cell Subclones

Masahide Uryu[1], Ayako Karino[2], Yukiko Kamihara[1], and Motohiro Horiuchi*[,1]

[1]*Laboratory of Prion Diseases, Graduate School of Veterinary Medicine, Hokkaido University, Sapporo, Hokkaido 060–0818, Japan, and* [2]*Department of Veterinary Public Health, Obihiro University of Agriculture and Veterinary Medicine, Obihiro, Hokkaido 080–8555, Japan*

Received January 31, 2007; in revised form, April 26, 2007. Accepted May 21, 2007

***Abstract*: In this study, we established Neuro2a (N2a) neuroblastoma subclones and characterized their susceptibility to prion infection. The N2a cells were treated with brain homogenates from mice infected with mouse prion strain Chandler. Of 31 N2a subclones, 19 were susceptible to prion as those cells became positive for abnormal isoform of prion protein (PrP^{Sc}) for up to 9 serial passages, and the remaining 12 subclones were classified as unsusceptible. The susceptible N2a subclones expressed cellular prion protein (PrP^{C}) at levels similar to the parental N2a cells. In contrast, there was a variation in PrP^{C} expression in unsusceptible N2a subclones. For example, subclone N2a-1 expressed PrP^{C} at the same level as the parental N2a cells and prion-susceptible subclones, whereas subclone N2a-24 expressed much lower levels of PrP mRNA and PrP^{C} than the parental N2a cells. There was no difference in the binding of PrP^{Sc} to prion-susceptible and unsusceptible N2a subclones regardless of their PrP^{C} expression level, suggesting that the binding of PrP^{Sc} to cells is not a major determinant for prion susceptibility. Stable expression of PrP^{C} did not confer susceptibility to prion in unsusceptible subclones. Furthermore, the existence of prion-unsusceptible N2a subclones that expressed PrP^{C} at levels similar to prion-susceptible subclones, indicated that a host factor(s) other than PrP^{C} and/or specific cellular microenvironments are required for the propagation of prion in N2a cells. The prion-susceptible and -unsusceptible N2a subclones established in this study should be useful for identifying the host factor(s) involved in the prion propagation.**

Key words: **Neuro2a, Prion, PrP, Susceptibility**

Transmissible spongiform encephalopathies, so-called prion diseases, are fatal neurodegenerative disorders that include scrapie in sheep and goats, bovine spongiform encephalopathy, and Creutzfeldt-Jakob disease in humans. The major component of causative agent of prion diseases, prion, is thought to be an abnormal isoform of prion protein (PrP^{Sc}). PrP^{Sc} is generated from a normal cellular prion protein (PrP^{C}) by certain post-translational modifications and the process in the conversion of PrP^{C} to PrP^{Sc} is considered to be a central event in pathogenesis of prion diseases (31). PrP^{C} is a sialo-glycoprotein expressed on the cell surface as a glycosyl-phosphatidylinositol anchoring protein (36). Cell biological studies have revealed that mature PrP^{C} on the cell surface acts as a substrate for the PrP^{Sc} biosynthesis, and formation of PrP^{Sc} takes place either at the cell membrane or during the endocytic pathway (3, 8, 37). Depletion of cholesterol inhibits PrP^{Sc} formation in prion-infected cells (2, 38), and the co-existence of PrP^{C} and PrP^{Sc} in lipid rafts or caveolae-like domains suggests that cholesterol- and sphingolipid-enriched membrane microdomains are sites for the interaction between PrP^{C} and PrP^{Sc} (29, 41).

Although PrP^{C} is essential for the propagation of prion and the development of prion diseases (6), other host factors are thought to be involved in the PrP^{Sc} formation, i.e., prion replication. Studies using chimeric

**Address correspondence to* Dr. Motohiro Horiuchi, Laboratory of Prion Diseases, Graduate School of Veterinary Medicine, Hokkaido University, Kita 18, Nishi 9, Kita-ku, Sapporo, Hokkaido 060–0818, Japan. Fax: +81–11–706–5293. E-mail: horiuchi@vetmed.hokudai.ac.jp

Abbreviations: CHO, Chinese hamster ovary; DMEM, Dulbecco's modified Eagle's medium; FBS, fetal bovine serum; GAPDH, glyceraldehyde-3-phosphate dehydrogenase; HS, heparan sulfate; LRP/LR, laminin receptor precursor/laminin receptor; MAb, monoclonal antibody; N2a, Neuro2a; PBS, phosphate-buffered saline; PrP, prion protein; PrP^{C}, cellular prion protein; PrP^{Sc}, abnormal isoform of prion protein; RT-PCR, reverse transcription-polymerase chain reaction; SDS-PAGE, sodium dodecyl sulfate-polyacrylamide gel electrophoresis; WB, Western blotting.

and point mutants of PrP have suggested that a host factor designated Protein X is required for prion propagation (18, 40), although its identity remains unknown. To date, Bcl-2 (21), laminin receptor precursor/laminin receptor (LRP/LR) (32), neural cell adhesion molecule (35), and several other proteins have been identified as possible counterparts of PrP^{C}. Plasminogen has been reported to bind PrP^{Sc} (11). In addition, a reduction in the level of LRP/LR inhibits PrP^{Sc} formation in prion-infected cells, suggesting that the LRP/LR has a direct or indirect role in prion propagation (22). The biological significance of other proteins in prion propagation remains unclear (34, 35).

Recently, cysteine proteases, such as calpain, and cathepsin B and L were reported to modulate PrP^{Sc} formation (23, 42). Furthermore, inhibitors of c-Abl tyrosine kinase and mitogen-activated protein kinase kinase are reported to accelerate PrP^{Sc} degradation in prion-infected cells (10, 30). Thus, changes in the cellular microenvironment, by interfering with cellular signaling, may also affect prion propagation. These findings suggest the involvement of other host factors for prion propagation. Identification of such host factors and cellular microenvironments involved in prion propagation is of great interest not only for understanding the basic mechanisms of prion propagation but also for finding new therapeutic targets.

Comparative analyses between permissive and non-permissive conditions for prion propagation will facilitate the identification of the host factors involved in prion propagation. In the present study, we established subclones of mouse Neuro2a (N2a) neuroblastoma cells and analyzed their susceptibility to prion. The prion-susceptible and -unsusceptible subclones established in this study should be useful for identifying host factors involved in prion replication.

Materials and Methods

Cell culture and cloning of the cells. N2a cell line (American Type Culture Collection CCL-131, 58th passage at the purchase) was grown in Dulbecco's modified Eagle's medium with high glucose (DMEM; ICN Biomedicals), 10% fetal bovine serum (FBS), and non-essential amino acids. N2a subclones were obtained by limiting dilution.

Inoculation of prion to N2a cells. Mouse prion strain Chandler was propagated in ICR mice (CLEA Japan, Inc.). The brains of mice at the terminal stage of the disease were homogenized in phosphate-buffered saline (PBS) at 10% (w/w) and the homogenates were stored at −30 C until use. The brain homogenate was diluted to 2% with the medium, and 500 μl was added to N2a cells in 60-mm dishes containing 1 ml of medium. After 24 hr, the medium was refreshed, and cells were serially passaged every 3 to 4 days at a 1:10 dilution.

Detection of PrP^{Sc}. Preparation and detection of PrP^{Sc} in the prion-infected cells were carried out as described previously (19, 20) with slight modifications. Cells were lysed in lysis buffer (0.5% Triton X-100, 0.5% sodium deoxycholate, 10 mM Tris-HCl, pH 7.5, 150 mM NaCl, and 5 mM EDTA), and small aliquots of the lysates were stored for the determination of the protein concentration. The remaining lysates were digested with 20 μg/ml proteinase K at 37 C for 20 min. The digestion was stopped by the addition of Pefabloc (Roche) to 5 mM. The mixture was adjusted to 0.3% phosphotungstic acid by addition of a 5% solution and then incubated for 30 min at 37 C with constant rotation. PrP^{Sc} was then collected by centrifugation at 20,000 × g for 20 min and subjected to SDS-PAGE followed by Western blotting (WB). Blots were probed with monoclonal antibody (mAb) 31C6 (20) and horseradish peroxidase-conjugated sheep $F(ab')_2$ fragment of anti-mouse IgG (Amersham Bioscience). The specific bands were visualized with ECL Western Blotting Detection Reagents (Amersham Bioscience) and a LAS-3000 chemiluminescence image analyzer (Fujifilm). Quantitative analyses of the blots were carried out with Image Reader LAS-3000 version 1.11 (Fujifilm).

Flow cytometry. Flow cytometric analysis was performed as described previously (19).

PrP^{Sc} binding assay. Cells were seeded at 2.5×10^4 cells/well in 6-well plates and grown for 48 hr. Cells were then fed with 500 μl of the fresh medium and inoculated with 250 μl of 0.4 to 2% prion-infected mouse brain homogenate diluted with medium, and kept for 3 hr at either 37 C or on ice with occasional tilting. After the incubation, cells were washed with PBS three times, and bound PrP^{Sc} was detected as described in detection of PrP^{Sc}.

Quantitative reverse transcription-polymerase chain reaction (RT-PCR) analysis. Total RNA was isolated from the cells with TRIzol Reagent (Invitrogen Life Technologies). First strand cDNA was synthesized from the total RNA using a First-Strand Synthesis Kit (Amersham Biosciences) according to the manufacturer's instructions. Real-time *Taq*Man PCR assays were performed to determine the relative quantity of mouse PrP gene expression. Amplification reaction mixtures contained template cDNA, 1X pre-designed set of primers and a *Taq*Man probe targeting the boundary between exons 1 and 2 of the PrP gene (*Taq*Man Gene Expression Assays No. Mm-00448389), and 1X *Taq*-

Man Universal PCR Master Mix (Applied Biosystems) in a final reaction volume of 20 μl. The amplification profile was monitored with an ABI PRISM 7900HT (Applied Biosystems), and the relative quantity was determined by the standard curve method (1) using SDS Plate Utility version 2.1 (Applied Biosystems). Expression of glyceraldehyde-3-phosphate dehydrogenase (GAPDH) gene was monitored as an endogenous control using *Taq*Man Rodent-GAPDH Control Reagents (Applied Biosystems).

Cellular cholesterol content of N2a subclones. Cells were seeded in 6-well plates in DMEM containing 10% FBS. After 48 hr, the medium was changed to Opti-MEM (Gibco) and cells were kept for additional 24 hr. Then, cells were washed three times with PBS and lysed with PBS containing 0.1% Triton X-100. The lysates were frozen at −30 C until use. The lysates were clarified by centrifugation at 20,000 × *g* for 15 min at 4 C, and the resulting supernatants were assayed for cholesterol using an Amplex Red Cholesterol Assay Kit (Molecular Probes) according to the manufacturer's instructions. Fluorescence was measured with a fluorescence microplate reader ARVO-SX (Wallac) using excitation at 560 nm and detection at 580 nm.

Stable expression of $MoPrP^C$. Eukaryotic expression vector, pRc/EF-MoPrP (M. H. and A. K. manuscript in preparation), which contains a mouse PrP cDNA expression unit driven by peptide chain elongation factor 1α promoter (27) along with the bacterial aminoglycoside phosphotransferase gene (G418 resistant gene) expression unit, was introduced into N2a cells with FuGENE 6 (Roche). The transfected cells were cultured in the presence of 0.3 mg/ml G418 (Gibco), and G418-resistant cells were selected. The cells were stained with anti-PrP mAb as described for the flow cytometric analysis (19), and cell sorting was performed using an EPICS ALTRA flow cytometer (Beckman Coulter). The cells with fluorescence intensities ranging from 100 to 500 were recovered and cultured with DMEM. Cells passaged more than 3 times were used for prion infection experiments.

Results

Prion-Susceptibility of N2a Subclones

We isolated 31 N2a subclones by limiting dilution and examined them for susceptibility to prion. The N2a subclones were inoculated with scrapie Chandler strain-infected mouse brain homogenates, and prion-susceptibility was determined by the presence of PrP^{Sc} during nine passages after inoculation. Figure 1 shows the representative results for PrP^{Sc} detection in the N2a subclones at the third, sixth, and ninth passages after inoculation. Of 31 N2a subclones, 19 (N2a-2, -3, -5, -6, -7, -17, -21, -22, and -25 in Fig. 1) were judged to be prion-susceptible, and the remaining 12 subclones (N2a-1, -4,

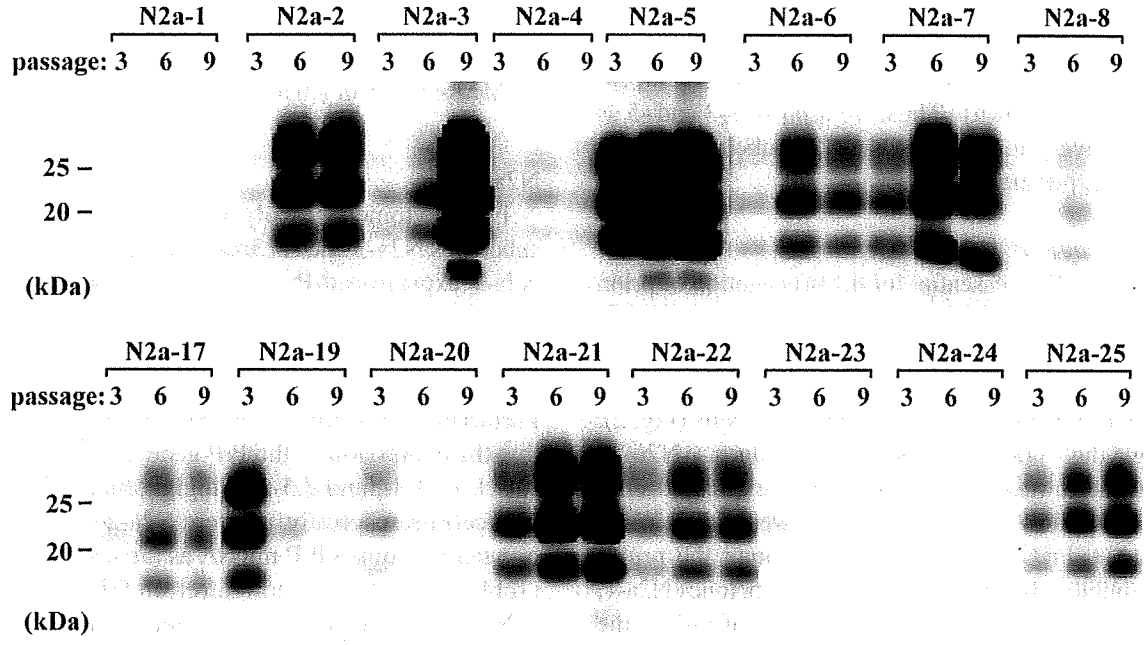

Fig. 1. Detection of PrP^{Sc} in N2a subclones inoculated with prion. N2a subclones were inoculated with 2% brain homogenate from mice infected with Chandler strain, and then consecutively passaged up to nine times. The presence of PrP^{Sc} was examined at the third, sixth, and ninth passages by WB. PrP^{Sc}-enriched sample derived from 0.1 mg of the cell lysates was loaded on each lane, and PrP^{Sc} was detected with mAb 31C6. Results of representative N2a subclones are indicated. Molecular markers are indicated on the left.

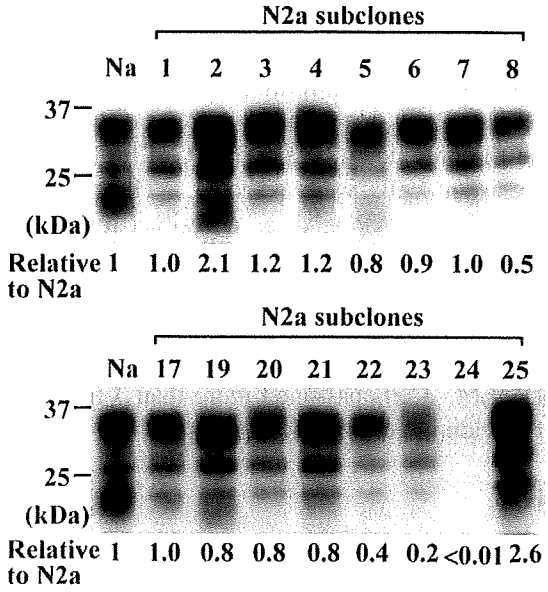

Fig. 2. Expression of PrP^C in N2a subclones. Ten micrograms of cell lysates were loaded on each lane, and PrP^C was detected with mAb 31C6. Na indicates parental N2a cells, and the numbers on the top of the images indicate the number of N2a subclones. Results of representative N2a subclones are indicated. The luminescence intensities were quantified with a LAS-3000 chemiluminescence image analyzer, and the numbers below the images indicate the mean PrP^C expression relative to that in the parental N2a cells (n = 2).

-8, -19, -20, -23, and -24 in Fig. 1) were classified as unsusceptible because they were negative for PrP^{Sc} at all passages examined. Subclones N2a-3 and -5, which showed intense PrP^{Sc} bands at the ninth passage (Fig. 1), were positive for PrP^{Sc} for more than 30 serial passages (data not shown). Thus, we used N2a-3 and -5 as representative prion-susceptible N2a subclones in the following experiments.

Expression of PrP^C and PrP Gene

Because PrP^C is essential for the propagation of prion and formation of PrP^{Sc} (5–7), we first investigated PrP^C expression in N2a subclones by WB (Fig. 2). As expected, prion-susceptible subclones expressed 0.4- to 2.6-fold as much PrP^C as the parental N2a cells (Fig. 2). Among the prion-susceptible subclones, N2a-22 showed the lowest PrP^C expression; it expressed only 0.4 ± 0.1-fold as much PrP^C as the parental N2a cells. In contrast, PrP^C expression varied among the prion-unsusceptible subclones. For instance, subclones N2a-1, -4, -8, -19, and -20 expressed similar level of PrP^C as the parental N2a cells and susceptible subclones, whereas N2a-23 and -24 had lower PrP^C expression than the parental cells, and actually, subclone N2a-24 expressed only one one-hundredth as much PrP^C as the parental N2a cells.

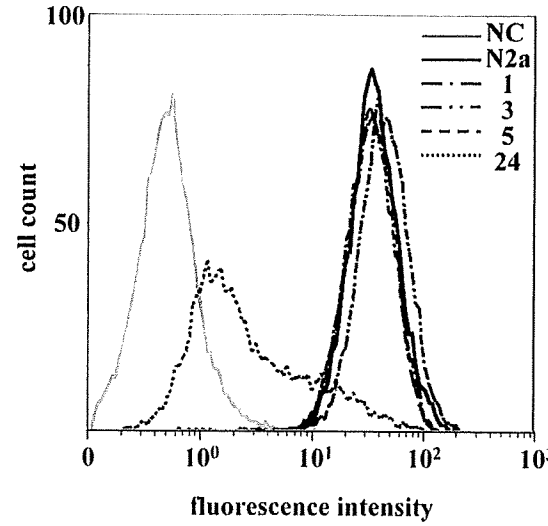

Fig. 3. Cell surface expression of PrP^C in N2a subclones. PrP^C on the cell surface of N2a and subclones N2a-1, -3, -5, and -24 was detected by flow cytometry. NC indicates the fluorescence intensity of N2a cells stained with negative control mAb P1-284 as a primary antibody. The PrP^C expression levels relative to that in parental N2a cells were calculated from mean fluorescence intensities and are shown in Table 1.

Table 1. Levels of PrP^C and PrP mRNA expression in N2a subclones

N2a subclone	Relative to parental N2a cells		
	Total PrP^C[a]	PrPC on cell surface[a]	PrP mRNA[a]
N2a-1	1.0 ± 0.7	1.1 ± 0.06	1.4 ± 0.4
N2a-3	1.2 ± 0.5	1.3 ± 0.07	1.8 ± 0.7
N2a-5	0.8 ± 0.2	1.0 ± 0.06	1.5 ± 0.4
N2a-24	0.01 ± 0.004	0.07 ± 0.006	0.1 ± 0.04

[a]Means ± S.D. (n=3) relative to parental N2a cells.

N2a cells.

Flow cytometric analysis showed that susceptible subclones N2a-3 and -5, and the unsusceptible subclone N2a-1 expressed PrP^C on their cell surfaces, whereas, consistent with the WB analysis, the level of PrP^C on the cell surface of the N2a-24 subclone was less than one-tenth of that in parental N2a cells (Fig. 3, Table 1). Furthermore, quantitative RT-PCR analysis also showed that the expression of the PrP gene in N2a-1, -3, and -5 was 1.4-, 1.8-, and 1.5-fold higher than in the parental N2a cells, respectively, whereas N2a-24 expressed only one-tenth as much PrP mRNA as the parental N2a cells (Table 1). Thus, the low level of PrP^C expression in N2a-24 is probably due to inefficient transcription of the PrP gene. These results indicated that there are two types of prion-unsusceptible N2a subclones: one (e.g., N2a-1) that expresses a level of PrP^C similar to prion-susceptible N2a cells, and another (e.g., N2a-24) that

expresses lower levels of PrP^C than susceptible cells.

Cellular Cholesterol Content of N2a Subclones

The cellular cholesterol is reported to be important for the accumulation of PrP^{Sc} in prion-infected N2a cells (2, 38). We therefore measured the cellular cholesterol content in representative N2a subclones; however, there was no significant difference in the cellular cholesterol contents between the parental N2a cells (8.3 ± 0.9 μg/mg protein), prion-unsusceptible subclones N2a-1 and -24 (8.6 ± 0.7 and 9.3 ± 0.9 μg/mg protein, respectively) and susceptible subclones N2a-3 and -5 (9.2 ± 0.4 and 7.9 ± 0.9 μg/mg protein, respectively).

Binding of PrP^{Sc} to N2a Subclones

Binding of PrP^{Sc} to the cells is considered to be the initial step in the prion infection after cells are inoculated with prion-infected brain homogenates. Thus, we examined the binding of PrP^{Sc} to N2a subclones to investigate whether the binding step is involved in determining the prion-susceptibility and whether the expression of PrP^C affects PrP^{Sc} binding. Figure 4a shows the representative results for the binding of PrP^{Sc} to N2a subclones at 37 C. PrP^{Sc} bound equally to prion-susceptible (N2a-3 and -5) and unsusceptible N2a subclones (N2a-1 and -24). In addition, there was no significant difference in the amount of bound PrP^{Sc} among N2a subclones and N2aII/9-4 that of stably overexpressed mouse PrP^C (Fig. 5a). In addition, we observed a dose-dependent increase in PrP^{Sc} binding both on ice and at 37 C, regardless of the prion susceptibility or level of PrP^C in the cells (Fig. 4b). The increase of bound PrP^{Sc} at 37 C suggests that a part of bound PrP^{Sc} may be internalized during the incubation. These results revealed that prion susceptibility of these subclones is not determined by the binding and/or uptake of PrP^{Sc} and that PrP^C is not directly involved in the binding and/or uptake of PrP^{Sc}.

Effect of Exogenously Introduced PrP^C on Prion Susceptibility

We speculated that the low level of PrP^C expression in N2a-24 may explain its inability to support prion replication. To examine this possibility, we transfected N2a-1 and -24 cells with the mouse PrP gene expression vector pRc/EF-MoPrP and selected stable transformants in the presence of G418. We also used the PrP^C-overexpressing N2a subclone N2aII/9-4, which is a stable transformant by pRc/EF-MoPrP, as a control for G418-resistant prion-susceptible cells. Quantitative analysis of

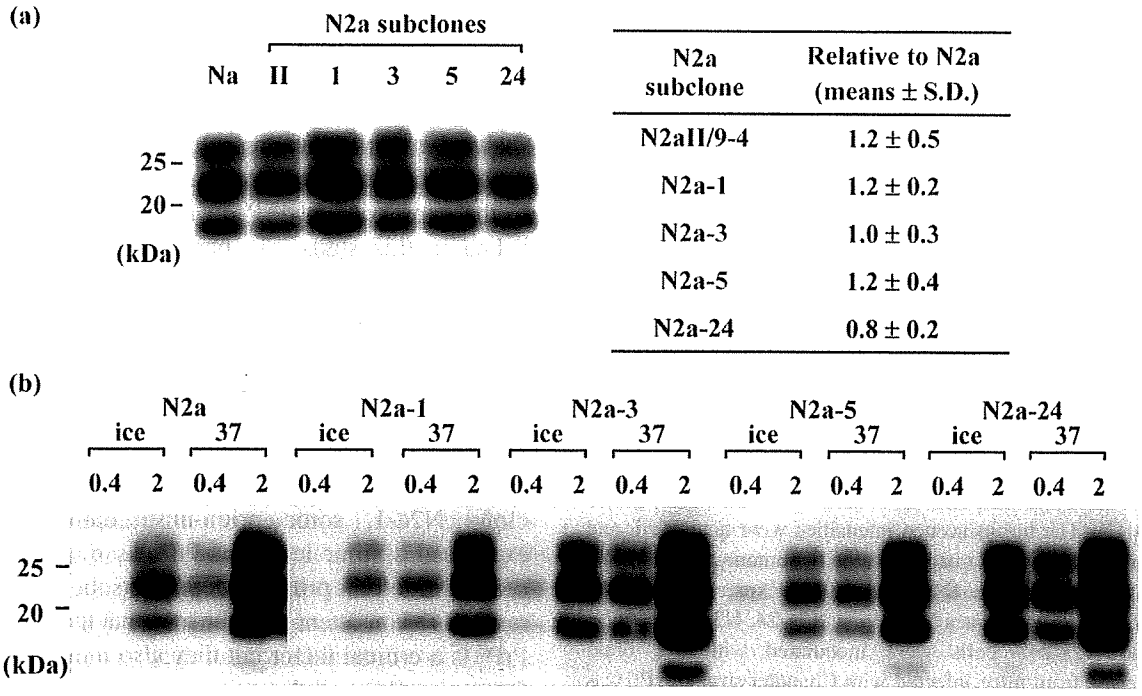

N2a subclone	Relative to N2a (means ± S.D.)
N2aII/9-4	1.2 ± 0.5
N2a-1	1.2 ± 0.2
N2a-3	1.0 ± 0.3
N2a-5	1.2 ± 0.4
N2a-24	0.8 ± 0.2

Fig. 4. Binding of PrP^{Sc} to N2a subclones. (a) Representative results for the binding of PrP^{Sc} to N2a cells. The cells were inoculated with 2% brain homogenate from mice infected with Chandler strain and then incubated at 37 C for 3 hr. Bound PrP^{Sc} was detected as described in "Materials and Methods." The binding of PrP^{Sc} relative to that in parental N2a cells is shown in the table on the right. Values in the table are the means ± S.D. from three independent experiments. Na, parental N2a cells; II, N2aII/9-4; 1, 3, 5, and 24, N2a subclone-1, -3, -5, and -24, respectively. (b) Dose- and temperature-dependent binding of PrP^{Sc}. The cells were inoculated with 0.4 and 2% brain homogenate from mice infected with Chandler strain and incubated at 37 C or on ice for 3 hr.

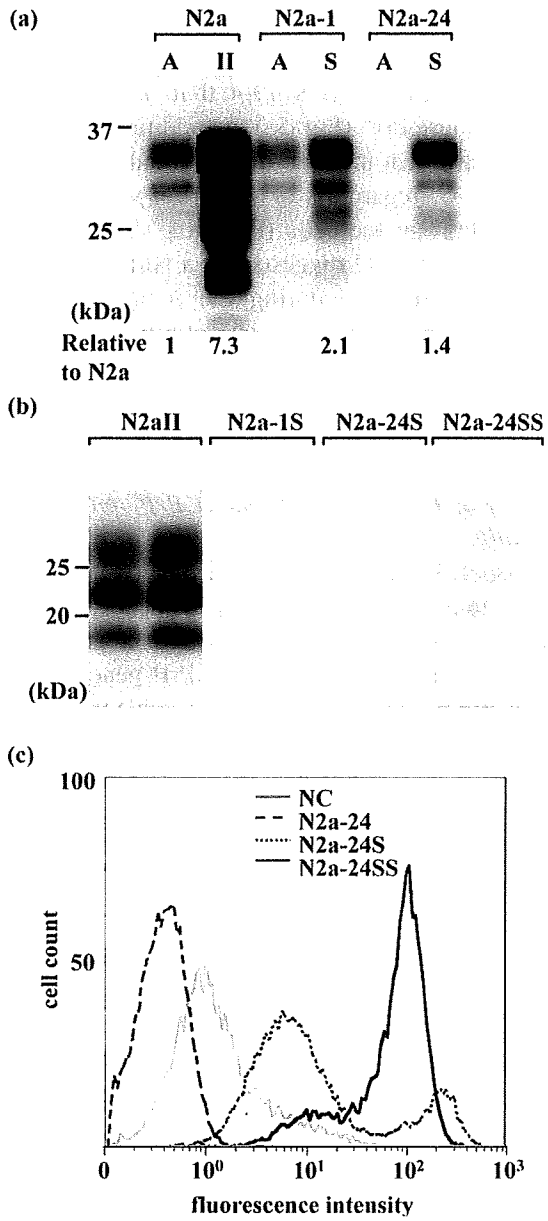

Fig. 5. (a) Expression of PrP^C in N2a, N2a-1, and N2a-24 cells. N2a-1 and N2a-24 subclones were transfected with pRc/EF-MoPrP, and G418-resistant cells were selected. A indicates authentic cells, and S indicates G418-resistant cells. The G418-resistant N2a subclone II/9-4 was used as a control for G418-resistant prion-susceptible cells. Ten micrograms of the cell lysates were loaded on each lane, and PrP^C was detected with mAb 31C6. The luminescence intensities were quantified, and the numbers below the image indicate the amount of PrP^C relative to that in N2a cells. (b) Effect of PrP^C expression on prion susceptibility of subclones N2a-1 and N2a-24. N2aII/9-4, N2a-1S, and N2a-24S cells were inoculated with 2% brain homogenate from mice infected with Chandler strain. PrP^{Sc} was detected after the sixth consecutive passage. The results of duplicate samples are shown. (c) Cell surface expression of PrP^C in N2a-24 cells. PrP^C on the cell surface of N2a-24, 24S, and 24SS (selected by cell sorter) was detected by flow cytometry. NC indicates the fluorescence intensity of N2a-24S cells stained with negative control mAb P1-284 as a primary antibody.

WB revealed that the G418-resistant N2a-1 (N2a-1S) and N2a-24 (N2a-24S) cells expressed 2.1- and 1.4-fold more PrP^C than the parental N2a cells (Fig. 5a). In addition, the G418-resistant N2a subclone N2aII/9-4 expressed 7.3-fold more PrP^C than parental N2a cells. Flow cytometric analysis revealed that 39% of N2a-1S (data not shown) and 32% of N2a-24S cells expressed higher surface level of PrP^C than the corresponding authentic subclones (Fig. 5c). These cells were inoculated with brain homogenate from prion-infected mice and then examined for PrP^{Sc} after six serial passages. PrP^{Sc} was detected in neither N2a-1S nor N2a-24S cells but was detected in N2aII/9-4 cells, suggesting that stable expression of PrP^C did not confer the prion susceptibility to N2a-1 and N2a-24 cells (Fig. 5b). The fact that 32% of G418-resistant N2a-24S cells expressed elevated levels of PrP^C might cause the inefficient prion replication in N2a-24S cells. To exclude this possibility, we collected PrP^C-overexpressing cells from G418-resistant N2a-24S cells by cell sorting. In this cell population (N2a-24SS), 79% of cells expressed elevated cell surface levels of PrP^C (Fig. 5c); however, PrP^{Sc} was not detected in these cells when they were inoculated with prion-infected brain homogenates (data not shown).

Discussion

N2a cells have been reported to be composed of cells with different susceptibilities to prion infection (4, 9). One of the determinants of prion susceptibility is the expression of PrP^C (3–5), but the quantitative relationship between PrP^C expression and prion susceptibility is not well understood. We found considerable variation in the expression of PrP^C in the N2a subclones established in this study. In particular, subclone N2a-24 expressed less than one one-hundredth as much PrP^C as the parental N2a cells. Among the prion-susceptible N2a subclones, N2a-22 showed the lowest expression of PrP^C but still expressed 0.4-fold as much PrP^C as the parental N2a cells, suggesting that a substantial amount of PrP^C is required to support prion propagation in N2a subclones. On the other hand, as represented by subclone N2a-1, some prion-unsusceptible subclones expressed similar levels of PrP^C as the parental N2a cells and other prion-susceptible subclones. These results are consistent with the idea that the expression of PrP^C is a critical factor but they also indicate that other factors and/or cellular microenvironments also determine the susceptibility of N2a cells to prion (4).

Exposing cells to prion-infected materials such as brain homogenates usually starts infection, and many cell lines can bind and internalize exogenous PrP^{Sc} (24, 25, 39). Recently, Hijazi et al. showed that the similar

levels of PrP^{Sc} bind to wild-type Chinese hamster ovary (CHO) cells, which do not express detectable levels of PrP^C, and CHO cells overexpressing PrP^C (13). Magalhaes et al. also showed that uptake of exogenous PrP^{Sc} does not require the presence of endogenous PrP^C (25). In agreement with these observations, our results indicated that the binding of exogenous PrP^{Sc} to the N2a cells was neither related to the prion susceptibility nor the level of PrP^C expression. This also indicated that the binding of PrP^{Sc} observed in this study did not account for the specific binding to PrP^C but binding of PrP^{Sc} to cell surface, although molecules and microenvironments involved in the binding are unclear. Cellular heparan sulfate (HS) has been reported to be involved in the uptake of exogenous PrP^{Sc} following productive prion propagation in cells (14). In addition, the complex of LRP/LR and HS proteoglycan has been suggested to act as a receptor for PrP^{Sc} (12, 15). We did not address the role of LRP/LR and HS proteoglycan in the binding of PrP^{Sc} to N2a subclones; however, when the binding assay was carried out at 37 C, PrP^{Sc} binding to the N2a subclones was increased regardless of the PrP expression level or prion susceptibility, suggesting that the uptake of PrP^{Sc} may not be a major determinant of prion susceptibility in the N2a subclones. A recent report showed that the trafficking of exogenous PrP^{Sc} in mouse septum neuron-derived SN56 cells differed according to the ability of prion to propagation in the cells (25). This suggested that prion susceptibility may be determined by events occurring after the uptake of PrP^{Sc}. Therefore it would be of interest to analyze the fate of PrP^{Sc} after its binding to prion-susceptible and -unsusceptible N2a subclones.

In this study, we obtained a subclone, N2a-24, in which the expression of PrP^C was much lower than in the parental N2a cells and other subclones. We confirmed that the low PrP^C expression was due to inefficient expression of PrP mRNA. To address whether the low level of PrP gene expression is caused by genomic mutations in the regions involved in transcription of the PrP gene, we used long PCR to amplify the 5′- and 3′-flanking regions of exon 1 (nucleotides 6055–12058 in accession number U29186), which contain regions influencing PrP gene expression (17, 33) and carried out a direct sequencing of the amplified products. We did not find any nucleotide differences in this region between authentic N2a cells and subclones N2a-5 and N2a-24. We further analyzed the nucleotide sequences of exon 3 and its flanking regions (nucleotides 27096–30189 in accession number U29186), but again, the sequences were identical in authentic N2a cells and subclones N2a-5 and N2a-24 (data not shown). Thus, the low level of PrP gene expression in N2a-24 was not due to a mutation in the PrP gene but rather was probably due to a deficiency in the cellular machinery used for transcription of the PrP gene. In hepatic stellate cells, which express trace amounts of PrP^C, the expression of PrP^C increased in response to CCl_4-induced hepatic damage (16). In addition, PrP^C expression is increased in peripheral nerves during axon regeneration (28). These studies raised the possibility that the regulation of PrP^C expression plays a role in neural and hepatic regeneration. In addition, PrP gene expression is developmentally regulated (26), but the molecular mechanism controlling PrP gene expression remains unclear. Thus, the low expression of the PrP gene in subclone N2a-24 despite a lack of mutations in the genomic region of the PrP gene, suggests that this subclone will be useful for analyzing the mechanism of PrP gene expression.

Host factors other than PrP^C may be involved in the PrP^{Sc} formation, i.e., prion replication, but little is known so far. A comparison of prion-susceptible and -resistant tissues could help to identify such host factors; however, large differences exist in gene expression profiles between tissues and thus comparison between tissues would complicate the identification of factors influencing prion susceptibility. A fine comparison would be possible, however, if the compared samples have similar biological properties. Hence, the N2a subclones established in this study should be useful for identifying host factors and cellular microenvironments influencing prion replication. Comprehensive comparison of these cells by transcriptomic and proteomic analyses will be useful in this regard and should help to elucidate the molecular mechanism of prion replication.

This work was supported by a grant from The 21st Century COE Program (A-1) and a Grant-in-Aid for Science Research (A) (grant 15208029) from the Ministry of Education, Culture, Sports, Science and Technology, Japan. This work was also supported by a grant from the Ministry of Health, Labour and Welfare, Japan.

References

1) Applied Biosystems: User Bulletin #2 ABI Prism 7700 Sequence Detection System: December 11, 1997.
2) Bate, C., Salmona, M., Diomede, L., and Williams, A. 2004. Squalestatin cures prion-infected neurons and protects against prion neurotoxicity. J. Biol. Chem. **279**: 14983–14990.
3) Borchelt, D.R., Scott, M., Taraboulos, A., Stahl, N., and Prusiner, S.B. 1990. Scrapie and cellular prion proteins differ in their kinetics of synthesis and topology in cultured cells. J. Cell Biol. **110**: 743–752.
4) Bosque, P.J., and Prusiner, S.B. 2000. Cultured cell sublines highly susceptible to prion infection. J. Virol. **74**:

4377–4386.
5) Brandner, S., Raeber, A., Sailer, A., Blattler, T., Fischer, M., Weissmann, C., and Aguzzi, A. 1996. Normal host prion protein (PrPC) is required for scrapie spread within the central nervous system. Proc. Natl. Acad. Sci. U.S.A. **93**: 13148–13151.
6) Büeler, H., Aguzzi, A., Sailer, A., Greiner, R.A., Autenried, P., Aguet, M., and Weissmann, C. 1993. Mice devoid of PrP are resistant to scrapie. Cell **73**: 1339–1347.
7) Büeler, H., Fisher, M., Lang, Y., Bluethmann, H., Lipp, H.P., DeArmond, S.J., Prusiner, S.B., Aguet, M., and Weissmann, C. 1992. Normal development and behavior of mice lacking the neuronal cell-surface PrP protein. Nature **356**: 577–582.
8) Caughey, B., and Raymond, G.J. 1991. The scrapie-associated form of PrP is made from a cell surface precursor that is both protease- and phospholipase-sensitive. J. Biol. Chem. **266**: 18217–18223.
9) Enari, M., Flechsig, E., and Weissmann, C. 2001. Scrapie prion protein accumulation by scrapie-infected neuroblastoma cells abrogated by exposure to a prion protein antibody. Proc. Natl. Acad. Sci. U.S.A. **98**: 9295–9299.
10) Ertmer, A., Gilch, S., Yun, S.W., Flechsig, E., Klebl, B., Stein-Gerlach, M., Klein, M.A., and Schatzl, H.M. 2004. The tyrosine kinase inhibitor STI571 induces cellular clearance of PrP(Sc) in prion-infected cells. J. Biol. Chem. **279**: 41918–41927.
11) Fischer, M.B., Roeckl, C., Parizek, P., Schwarz, H.P., and Aguzzi, A. 2000. Binding of disease-associated prion protein to plasminogen. Nature **408**: 479–483.
12) Gauczynski, S., Nikles, D., El-Gogo, S., Papy-Garcia, D., Rey, C., Alban, S., Barritault, D., Lasmezas, C.I., and Weiss, S. 2006. The 37-kDa/67-kDa laminin receptor acts as a receptor for infectious prions and is inhibited by polysulfated glycanes. J. Infect. Dis. **194**: 702–709.
13) Hijazi, N., Kariv-Inbal, Z., Gasset, M., and Gabizon, R. 2005. PrPSc incorporation to cells requires endogenous glycosaminoglycan expression. J. Biol. Chem. **280**: 17057–17061.
14) Horonchik, L., Tzaban, S., Ben-Zaken, O., Yedidia, Y., Rouvinski, A., Papy-Garcia, D., Barritault, D., Vlodavsky, I., and Taraboulos, A. 2005. Heparan sulfate is a cellular receptor for purified infectious prions. J. Biol. Chem. **280**: 17062–17067.
15) Hundt, C., Peyrin, J.M., Haik, S., Gauczynski, S., Leucht, C., Rieger, R., Riley, M.L., Deslys, J.P., Dormont, D., Lasmezas, C.I., and Weiss, S. 2001. Identification of interaction domains of the prion protein with its 37-kDa/67-kDa laminin receptor. EMBO J. **20**: 5876–5886.
16) Ikeda, K., Kawada, N., Wang, Y.Q., Kadoya, H., Nakatani, K., Sato, M., and Kaneda, K. 1998. Expression of cellular prion protein in activated hepatic stellate cells. Am. J. Pathol. **153**: 1695–1700.
17) Inoue, S., Tanaka, M., Horiuchi, M., Ishiguro, N., and Shinagawa, M. 1997. Characterization of the bovine prion protein gene: the expression requires interaction between the promoter and intron. J. Vet. Med. Sci. **59**: 175–183.
18) Kaneko, K., Zulianello, L., Scott, M., Cooper, C.M., Wallace, A.C., James, T.L., Cohen, F.E., and Prusiner, S.B. 1997. Evidence for protein X binding to a discontinuous epitope on the cellular prion protein during scrapie prion propagation. Proc. Natl. Acad. Sci. U.S.A. **94**: 10069–10074.
19) Kim, C.L., Karino, A., Ishiguro, N., Shinagawa, M., Sato, M., and Horiuchi, M. 2004. Cell-surface retention of PrP(C) by anti-PrP antibody prevents protenase-resistant PrP formation. J. Gen. Virol. **85**: 3473–3482.
20) Kim, C.L., Umetani, A., Matui, T., Ishiguro, N., Shinagawa, M., and Horiuchi, M. 2004. Antigenic characterization of an abnormal isoform of prion protein using a new diverse panel of monoclonal antibodies. Virology **320**: 40–51.
21) Kurschner, C., and Morgan, J.I. 1995. The cellular prion protein (PrP) selectively binds to Bcl-2 in the yeast two-hybrid system. Brain Res. Mol. Brain Res. **30**: 165–168.
22) Leucht, C., Simoneau, S., Rey, C., Vana, K., Rieger, R., Lasmezas, C.I., and Weiss, S. 2003. The 37 kDa/67 kDa laminin receptor is required for PrP(Sc) propagation in scrapie-infected neuronal cells. EMBO Rep. **4**: 290–295.
23) Luhr, K.M., Nordstrom, E.K., Low, P., and Kristensson, K. 2004. Cathepsin B and L are involved in degradation of prions in GT1-1 neuronal cells. NeuroReport **15**: 1663–1667.
24) Luhr, K.M., Wallin, R.P., Ljunggren, H.G., Low, P., Taraboulos, A., and Kristensson, K. 2002. Processing and degradation of exogenous prion protein by CD11c(+) myeloid dendritic cells *in vitro*. J. Virol. **76**: 12259–12264.
25) Magalhaes, A.C., Baron, G.S., Lee, K.S., Steele-Mortimer, O., Dorward, D., Prado, M.A., and Caughey, B. 2005. Uptake and neuritic transport of scrapie prion protein coincident with infection of neuronal cells. J. Neurosci. **25**: 5207–5216.
26) Manson, J., West, J.D., Thomson, V., McBride, P., Kaufman, M.H., and Hope, J. 1992. The prion protein gene: a role in mouse embryogenesis? Development **115**: 117–122.
27) Mizushima, S., and Nagata, S. 1990. pEF-BOS, a powerful mammalian expression vector. Nucleic Acids Res. **18**: 5322.
28) Moya, K.L., Hassig, R., Breen, K.C., Volland, H., and Di Giamberardino, L. 2005. Axonal transport of the cellular prion protein is increased during axon regeneration. J. Neurochem. **92**: 1044–1053.
29) Naslavsky, N., Stein, R., Yanai, A., Friedlander, G., and Taraboulos, A. 1997. Characterization of detergent-insoluble complexes containing the cellular prion protein and its scrapie isoform. J. Biol. Chem. **272**: 6324–6331.
30) Nordstrom, E.K., Luhr, K.M., Ibanez, C., and Kristensson, K. 2005. Inhibitors of the mitogen-activated protein kinase kinase 1/2 signaling pathway clear prion-infected cells from PrPSc. J. Neurosci. **25**: 8451–8456.
31) Prusiner, S.B. 1991. Molecular biology of prion diseases. Science **252**: 1515–1522.
32) Rieger, R., Edenhofer, F., Lasmezas, C.I., and Weiss, S. 1997. The human 37-kDa laminin receptor precursor interacts with the prion protein in eukaryotic cells. Nat. Med. **3**: 1383–1388.
33) Saeki, K., Matsumoto, Y., Matsumoto, Y., and Onodera, T. 1996. Identification of a promoter region in the rat prion protein gene. Biochem. Biophys. Res. Commun. **219**:

47–52.
34) Salmona, M., Capobianco, R., Colombo, L., De Luigi, A., Rossi, G., Mangieri, M., Giaccone, G., Quaglio, E., Chiesa, R., Donati, M.B., Tagliavini, F., and Forloni, G. 2005. Role of plasminogen in propagation of scrapie. J. Virol. **79**: 11225–11230.
35) Schmitt-Ulms, G., Legname, G., Baldwin, M.A., Ball, H.L., Bradon, N., Bosque, P.J., Crossin, K.L., Edelman, G.M., DeArmond, S.J., Cohen, F.E., and Prusiner, S.B. 2001. Binding of neural cell adhesion molecules (N-CAMs) to the cellular prion protein. J. Mol. Biol. **314**: 1209–1225.
36) Stahl, N., Borchelt, D.R., and Prusiner, S.B. 1990. Differential release of cellular and scrapie prion proteins from cellular membranes by phosphatidylinositol-specific phospholipase C. Biochemistry **29**: 5405–5412.
37) Taraboulos, A., Raeber, A.J., Borchelt, D.R., Serban, D., and Prusiner, S.B. 1992. Synthesis and trafficking of prion proteins in cultured cells. Mol. Biol. Cell **3**: 851–863.
38) Taraboulos, A., Scott, M., Semenov, A., Avrahami, D., Laszlo, L., and Prusiner, S.B. 1995. Cholesterol depletion and modification of COOH-terminal targeting sequence of the prion protein inhibit formation of the scrapie isoform. J. Cell Biol. **129**: 121–132.
39) Taraboulos, A., Serban, D., and Prusiner, S.B. 1990. Scrapie prion proteins accumulate in the cytoplasm of persistently infected cultured cells. J. Cell Biol. **110**: 2117–2132.
40) Telling, G.C., Scott, M., Mastrianni, J., Gabizon, R., Torchia, M., Cohen, F.E., DeArmond, S.J., and Prusiner, S.B. 1995. Prion propagation in mice expressing human and chimeric PrP transgenes implicates the interaction of cellular PrP with another protein. Cell **83**: 79–90.
41) Vey, M., Pilkuhn, S., Wille, H., Nixon, R., DeArmond, S.J., Smart, E.J., Anderson, R.G., Taraboulos, A., and Prusiner, S.B. 1996. Subcellular colocalization of the cellular and scrapie prion proteins in caveolae-like membranous domains. Proc. Natl. Acad. Sci. U.S.A. **93**: 14945–14949.
42) Yadavalli, R., Guttmann, R.P., Seward, T., Centers, A.P., Williamson, R.A., and Telling, G.C. 2004. Calpain-dependent endoproteolytic cleavage of PrPSc modulates scrapie prion propagation. J. Biol. Chem. **279**: 21948–21956.

FULL PAPER *Public Health*

Evaluation of Methods for Removing Central Nervous System Tissue Contamination from the Surface of Beef Carcasses after Splitting

Naoko TAKADA[1)], Motohiro HORIUCHI[2)], Tetsutaro SATA[3)] and Yasushi SAWADA[1)]

[1)]Shibaura Meat Sanitary Inspection Station, Bureau of Social Welfare and Public Health, Tokyo Metropolitan Government, 2–17–19 Kounan, Minato-ku, Tokyo 108–0075, [2)]Laboratory of Prion Diseases, Graduate School of Veterinary Medicine, Hokkaido University, Kita 18, Nishi 9, Kita-ku, Sapporo 060–0818 and [3)]Department of Pathology, National Institute of Infectious Diseases, Toyama 1–23–1, Shinjuku-ku, Tokyo 162–8640, Japan

(Received 1 May 2008/Accepted 11 June 2008)

ABSTRACT. Since high levels of prions, the causative agent of bovine spongiform encephalopathy (BSE), accumulate in the brain and spinal cord, contamination of beef carcasses with central nervous system tissue (CNST) may occur at post-slaughter process. In this study, we investigated CNST contamination on the surface of beef carcasses using glial fibrillary acidic protein as a marker after splitting and evaluated the effects of washing procedures on contamination removal. High levels of CNST contamination was detected immediately after splitting, especially in the area close to the spinal column. This suggests that spinal cord fragments are attached to carcasses at the time of splitting even though the spinal cords have been removed by vacuum before splitting. Steam cleaning or manually washing with normal pressure water around the spinal column, performed prior to washing with high-pressure water, was found to be effective for reducing the level of CNST contamination. Furthermore, manually washing with high-pressure water could reduce CNST contamination to almost negligible levels. These results are useful for preparation of appropriate sanitation standard operating procedures to reduce the risk of CNST contamination of carcasses for prevention of exposure to BSE prion via the food chain.

KEY WORDS: BSE, carcass splitting, central nervous system tissues, glial fibrillary acidic protein, post-slaughter.

J. Vet. Med. Sci. 70(11): 1225–1230, 2008

Since the epidemiological linkage of bovine spongiform encephalopathy (BSE) to the occurrence of variant Creutzfeldt-Jakob disease in human was reported, BSE has been recognized as a foodborne disease [13]. Prion infectivity exists abundantly in the brain and spinal cord of BSE-affected cattle. BSE prion has also been detected in the trigeminal ganglion, dorsal root ganglia and, though at low levels, peripheral tissues such as the retina, bone marrow, tonsil and distal ileum [2, 11, 12]. The brain, spinal column including the spinal cord and dorsal root ganglia and distal ileum are removed as specified risk materials (SRMs) and thus kept out of the chain of consumption to reduce the risk of foodborne BSE infection. Recently, the existence of prion in tissues other than SRMs became evident; an abnormal isoform of prion protein, PrP^{Sc}, which is thought to be a major component of prion, was detected in the peripheral nerves [5] and adrenal glands of BSE-affected cattle [7].

There are reports of carcasses and meat products contaminated with CNST in spite of washing [6, 8, 14]. These reports determined the levels of CNST using glial fibrillary acidic protein (GFAP) as a marker and indicated that carcasses were contaminated with CNST under the following conditions: (1) brain tissue, destroyed by penetrating captive bolt stunning or pithing, is carried into muscle tissue via blood flow [1, 3]; (2) spinal cord fragments are attached to the surface of carcasses during splitting [4]; and (3) carcass washing after splitting is insufficient to remove spinal cord fragments from the carcass surface [8]. In addition, cross-contamination from SRM-contaminated carcasses is also a potential source of contamination [8].

In this collaborative study of 8 slaughterhouses in Japan, we investigated CNST contamination on the surface of the carcasses using GFAP as a marker for CNST. First, we investigated the contamination of carcasses with CNST immediately after splitting to understand the actual situation of contamination in Japan. Contamination was detected at all slaughterhouses examined, although the positive rate and degree of contamination varied among the slaughterhouses. Carcasses must be rid of CNST contamination in slaughterhouses before they are shipped as food products. Herein, we report the level of CNST contamination and effectiveness of washing procedures for removing CNST contamination on the beef carcass.

MATERIALS AND METHODS

Slaughtering process and analysis objectives: This study was conducted at eight domestic slaughterhouses (A-H) between August and November 2006. The general slaughtering process is outlined in Fig. 1A. Following stunning, exsanguination, and head removal, the carcasses were hung up by the hind legs. A tube was inserted into the spinal canal to suck out the spinal cord, and then the carcass was split. The carcasses were subsequently washed automatically or manually with high-pressure water. Prior to washing with high-pressure water, either steam cleaning or manual washing with normal-pressure water was carried out

* CORRESPONDENCE TO: SAWADA, Y., Shibaura Meat Sanitary Inspection Station, Bureau of Social Welfare and Public Health, Tokyo Metropolitan Government, 2–17–19 Kounan, Minato-ku, Tokyo 108–0075, Japan.
e-mail: Yasushi_Sawada@member.metro.tokyo.jp

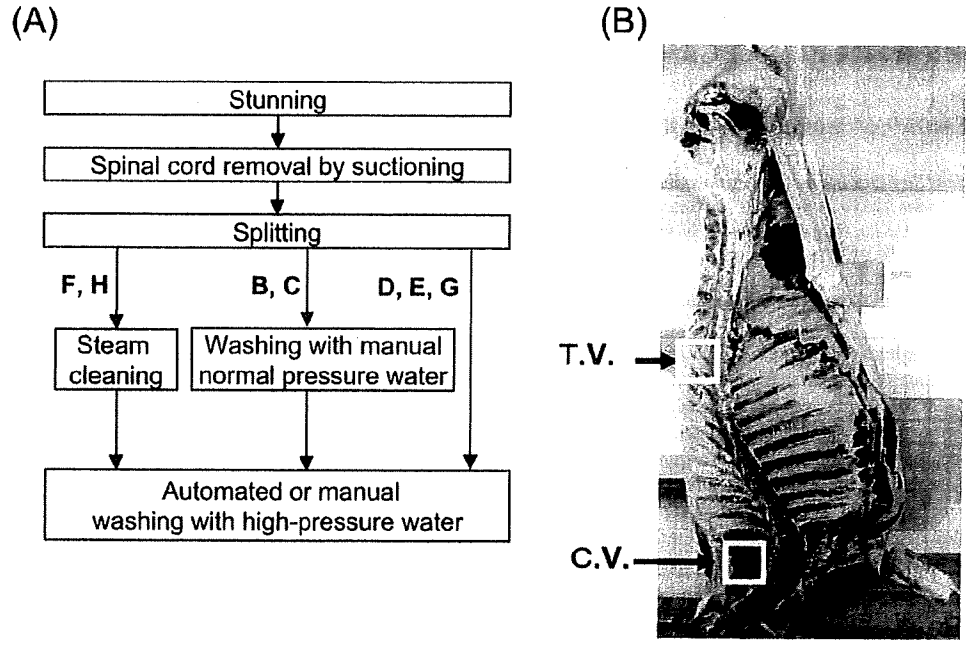

Fig. 1. Slaughtering process (A) and area for sampling (B). The effects of steam cleaning, washing with normal pressure water and manual washing with high-pressure water on the removal of CNST contamination from the surfaces of carcasses were evaluated at shaughterhouses F and H, B and C and D, E and G, respectively. C.V. and T.V. indicate the third cervical and last thoracic vertebra areas for sampling. One hundred cm^2 (10 cm x 10 cm) sections were wiped in the respective areas.

as preliminary washing to ensure the efficacy of high-pressure washing. At the time of planning of this research, most of slaughterhouses manually washed carcasses with high-pressure water without a preliminary washing step. Therefore, this study was designed to first investigate the actual situation of CNST contamination on the surface of carcasses immediately after splitting (at slaughterhouses A to H). Next, we attempted to evaluate the effects of steam cleaning (at slaughterhouses F and H) and manual washing with normal-pressure water (at slaughterhouses B and C) on CNST removal as a preliminary washing step and the effect of manual washing with high-pressure water on the CNST removal as the main washing step.

GFAP detection by enzyme immunoassay: One hundred square centimeters of sectioned muscle or fat on the split surface of wet carcasses were wiped off with dry sterile cotton applicators around the third cervical vertebra or last thoracic vertebra (Fig. 1B). The swabs of the applicators carrying the wiped-off materials were put into 2 m*l* sterile tubes for immediate laboratory testing.

Ridascreen Risk Material 10/5 (R-Biopharm GmbH, Germany), an ELISA-based test, was used to detect GFAP in the wiped-off samples. Following the manufacturer's instructions, the levels of CNST in the samples were determined from standard curves and were expressed as GFAP amounts per 100 cm^2. Samples with a GFAP concentration above 3 *n*g/100 cm^2, the detection limit of the kit used, were judged to be positive. Data analysis was performed assuming that GFAP concentrations below the detection limit were equal to 0 *n*g/100 cm^2. If the GFAP concentration exceeded the quantitation range, the sample was diluted for remeasurement and subsequent calculation of the actual GFAP concentration in consideration of the dilution ratio.

RESULTS

Residual CNST on the carcass surface immediately after splitting: Beef carcasses were investigated immediately after splitting in eight slaughterhouses to determine the levels of residual CNST on their surfaces (Table 1). Among these slaughterhouses, slaughterhouse D, which did not withdraw the spinal cord by suction, showed the highest GFAP positive rate (100%) around both the third cervical vertebra and last thoracic vertebra. The other slaughterhouses, at which the spinal cord was withdrawn by suction before splitting, showed GFAP positive rates ranging from 21.7 to 85.0%. In contrast, the residual levels of CNST exceeded 1 μg/100 cm^2 around the third cervical vertebra in slaughterhouse C and around the last thoracic vertebra in slaughterhouses B and H. This suggests that the level of contamination may not depend on removal of spinal cord, but instead scattering of saw residue during splitting may cause contamination in a limited area. Thus, removal of the scattered residue by washing is essential to reduce contami-

Table 1. Residual levels of CNST immediately after splitting

Slaughterhouse	Wiped section[a)]	n	Positive rate (%)	GFAP (*ng*/100 cm^2)			
				Mean	Standard deviation	Maximum	Minimum
A	C.V.	60	21.7	2.4	5.7	29.6	<3
	T.V.	60	73.3	22.3	31.4	178.3	<3
B	C.V.	20	85	89	150.3	651.8	<3
	T.V.	20	70	156.3	283.1	1,076.40	<3
C	C.V.	70	32.9	27.6	138.5	1,112.30	<3
	T.V.	70	42.9	19.4	80.2	578	<3
D	C.V.	111	100	49.6	49.1	303.5	3.3
	T.V.	111	100	149.6	132.6	490.9	10.2
E	C.V.	40	30	5.7	10.3	36.1	<3
	T.V.	40	22.5	12	28.2	121.8	<3
F	C.V.	55	43.6	8.7	26.5	190.6	<3
G	C.V.	40	45	9.8	27.9	168.7	<3
	T.V.	40	52.5	16.9	32	161.3	<3
H	C.V.	100	44	36.4	91	648.8	<3
	T.V.	100	24	32.2	152.2	1,328.40	<3

a) C.V. and T.V. indicate the third cervical and last thoracic vertebra areas, respectively.

Table 2. Effects of steam cleaning[a)]

Slaughterhouse	Wiped section[b)]	n	GFAP concentration (*ng*/100 cm^2)						Rate of decrease (%)
			Before steam cleaning			After steam cleaning			
			Mean	Maximum	Minimum	Mean	Maximum	Minimum	
F	C.V.	20	11.7	190.6	<3	3.4	51.2	<3	70.9
H	C.V.	100	36.4	648.8	3.9	13.6	348.2	3.4	62.6
	T.V.	100	32.2	1,328.4	3.4	18.4	493.0	3.5	42.9

a) Steam Vacuum System Model CV-1 (Jarvis, USA) was used.
b) C.V. and T.V. indicate the third cervical and last thoracic vertebra areas, respectively.

Table 3. Effects of manual washing with normal pressure water[a)]

Slaughterhouse	Wiped section	n	GFAP concentration (*ng*/100 cm^2)						Rate of decrease (%)
			Before washing			After washing			
			Mean	Maximum	Minimum	Mean	Maximum	Minimum	
B	C.V.	20	115.8	651.8	<3	21.7	73.9	<3	81.3
	T.V.	20	155.4	1,076.4	<3	17.2	116.8	<3	88.9
C	C.V.	10	115.1	1,112.3	<3	0.8	4.6	<3	99.3
	T.V.	10	63.1	578.0	<3	15.6	106.6	<3	75.3

a) The entire split surfaces of carcasses were washed evenly for 15 seconds.

nation of carcasses with CNST.

Effects of steam cleaning on CNST removal: The effects of steam cleaning on CNST removal were examined in slaughterhouses F and H. Steam cleaning was performed by spraying the surfaces of carcasses with approximately 80°C steam and simultaneously sucking substances attached to the surface of the carcasses through a suction nozzle moving across the carcass surface. Table 2 shows the mean levels of CNST residue before and after steam cleaning and the corresponding rate of decrease. In addition, the maximum and minimum levels of CNST residue are also indicated. In each slaughterhouse, the maximum levels of CNST residue decreased after washing. All cases showed a 42.9 to 70.9% decrease in the mean CNST levels after steam cleaning, demonstrating that this treatment is effective for removing CNST residue attached to carcasses.

Effects of manual washing with normal pressure water on CNST removal: The effects of manual washing with normal pressure water on CNST removal were examined in slaughterhouses B and C. The entire split surfaces of carcasses were washed evenly for 15 seconds. Table 3 shows the mean levels of residual CNST before and after washing and

the corresponding rate of decrease after washing. The maximum levels of CNST residue decreased after washing, and both slaughterhouses showed a decreases in the mean CNST levels of more than 75% after manual washing with normal pressure water, demonstrating that this treatment is also effective for CNST removal from carcasses.

Effects of manual washing with high-pressure water on CNST removal: In Japan, slaughterhouses generally conduct manual washing of carcasses with high-pressure water using a gun-type nozzle if automatic high-pressure washers are not available. At present, more than 60% of slaughterhouses have introduced manual washing with high-pressure water (unpublished observation). Therefore, the effects of manual washing with high-pressure water on CNST removal were examined in slaughterhouses D, E and G. Ebara Pressure washers (Ebara Corp., Japan), Plunger Pump units (Arimitsu Industry Co., Ltd., Japan) and Rocky washers (Arimitsu Industry Co., Ltd., Japan) were used in slaughterhouses D, E and G, respectively.

Figure 2 shows the changes in the average levels of CNST residue during manual washing with high-pressure water. In slaughterhouse D, the average residue level of CNST around the last thoracic vertebra was as high as 159.7 *ng*/100 cm^2 before washing, but decreased to 24.7 *ng*/100 cm^2 after washing for 15 seconds and then to 3.4 *ng*/100 cm^2 after washing for 60 sec. Similarly, the average CNST residue level around the third cervical vertebra was as high as 59.3 *ng*/100 cm^2 before washing, but decreased to 19.7 *ng*/100 cm^2 after washing for 15 sec and then to 4.8 *ng*/100 cm^2 after washing for 60 sec (Fig. 2A). In slaughterhouse E, the average CNST residue levels were relatively low before washing (12.1 *ng*/100 cm^2 around the last thoracic vertebra and 5.7 *ng*/100 cm^2 around the third cervical vertebra). The levels fell below the detection limit around the last thoracic vertebra after washing for 45 sec and around the third cervical vertebra after washing for 30 sec.

We also examined the efficacy of manual washing with high-pressure water in terms of washing order (Fig. 2B). In slaughterhouse G, the upper part of the split surfaces of carcasses in particular were washed for 40 sec and then the lower parts of the split surfaces of some of the carcasses were washed intensively for 30 or 45 sec. The average CNST levels around the third cervical vertebra before washing, 8.1 *ng*/100 cm^2, increased to 14.4 *ng*/100 cm^2 when only the upper part of the carcass was washed, but decreased below the detection limit when the lower part of the carcass was also washed for at least 45 sec. The average CNST residue level around the last thoracic vertebra, which was 7.1 *ng*/100 cm^2 before washing, decreased significantly even when only the upper carcass was washed and decreased below the detection limit when the lower section of the carcass was also washed.

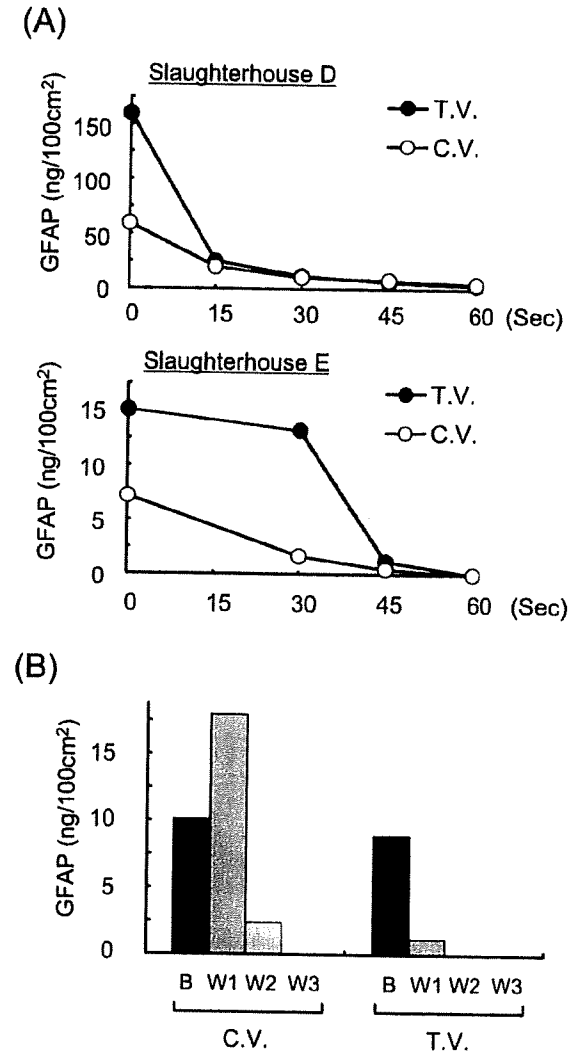

Fig. 2. Effect of manual washing with high-pressure water on removal of CNST contamination. (A) Evaluation of duration of washing. Zero indicates the GFAP levels before washing, and the GFAP levels after washing for 15 to 60 sec were plotted. The graphs show the average of 10 samples. C.V. and T.V. indicate the third cervical and the last thoracic vertebra areas for sampling. (B) Effect of the order of washing. Three washing protocols (W1 to W3) were tested for removal of CNST fragments from the carcasses. B, before washing; W1, washing only the upper parts of carcasses for 40 sec; W2, washing of the upper parts for 40 seconds and subsequent washing of the lower parts for 30 sec; W3, washing of the upper parts for 40 sec and subsequent washing of the lower parts for 40 sec. The graph shows the averages for 20 samples.

DISCUSSION

There are several reports available concerning CNST contamination on the surface of carcasses after high-pressure washing in slaughterhouses. Prendergast *et al.* [8] reported high contamination near the splitting line on the internal surfaces of carcasses, and Lim *et al.* [6] reported that the internal surfaces of carcasses were more contaminated than the external surfaces. According to their findings, they believe that contamination on the surface of

carcasses depends not only on the slaughtering method but also on the splitting or washing method. According to Prendergast *et al.* [9], the longer splitting takes, the larger the amount of sawing residue accumulation on the blade and thus the greater the CNST contamination of the carcass.

In the present study, we showed that the degree of CNST contamination was higher in a slaughterhouse where the spinal cord was not removed before splitting than in those where the spinal cord was removed before splitting. Thus, removal of the spinal cord before splitting is believed to be effective in reducing the occurrence of CNST contamination during splitting. Similarly, Helps *et al.* [4] reported that CNST contamination on the carcass surface is reduced by removal of the spinal column with an experimental oval saw that can remove it without exposing the spinal cord. These reports indicate that spinal cord suction plays a role in reducing the risk of CNST contamination of carcasses. However, it is difficult to completely remove the spinal cord by suction, and substantial amount of residual spinal cord and dura matter still remain in the spinal column after suction. In fact, we showed that the residual levels of CNST varied greatly from over 1 μg/100 cm^2 to below the detection limit, even though the spinal cord was removed by vacuum before splitting. Such contamination on the surfaces of carcasses is possibly due to scattering of spinal cord fragments remaining in the spinal columns as sawing residue, as pointed out by Ramantanis [7]. Thus, adequate washing of carcasses after splitting is indispensable for reducing the risk of CNST contamination.

Steam cleaning and manual washing with normal pressure water are 2 possible methods of ensuring the efficacy of washing with high-pressure water in terms of reducing CNST contamination. In this study, we showed that both methods are useful in reducing the residual levels of CNST but that they cannot completely remove them. Steam cleaning, unlike washing with high-pressure water, does not scatter pieces of tissue, and therefore, it appears to be useful especially in removing spinal cord and dura mater fragments attached around the spinal column without scattering them. Helps *et al.* [4] reported that steam cleaning would contribute to dissemination of CNST fragments onto the external surface of carcasses by movement of the nozzle. During steam cleaning, the nozzle should not be moved from the internal surface to the external surface of the carcass and must be washed after cleaning of each carcass to prevent spread of CNST via the nozzle itself. As a preliminary washing procedure, washing with normal pressure water can be easily introduced without any special changes in the slaughtering line or installation of expensive equipment. Also, washing with normal pressure water is advantageous for preventing the spread of contamination because it scatters less water than manual washing with high-pressure water.

As shown in Fig. 2, manual washing with high-pressure water for 60 seconds can reduce even large amounts of residual CNST to nearly below the detection limit. However, the levels of CNST residue around the third cervical vertebra increased if only the upper part of the carcass was washed (Fig. 2B). This is probably due to CNST dripping down to the third cervical vertebra area when the carcasses were hung up by the hind legs. Therefore, in order to reduce CNST contamination below the detection level, it is important to perform washing in the correct order and for the appropriate duration. In addition, it is necessary to separate the washing area from the surroundings to prevent spread of CNST via the water if washing with high-pressure water is adopted.

It is important to understand the effect of the washing methods on CNST removal in order to choose a method that works properly. In the present study, we reported the actual situation of contamination of carcasses by CNST and showed the effects of different methods of carcass cleaning on CNST removal. Our results suggest an efficient method for removal of CNST contamination from the surface of carcasses. To minimize CNST contamination on the surface of carcasses, vacuum removal of the spinal cord is a prerequisite. High levels of CNST contamination, possibly caused by splitting, should be reduced by a preliminary washing step such as steam cleaning or washing with normal pressure water, and washing with high-pressure water should then be performed to reduce the CNST contamination to a negligible level. We believe that these results will provide useful information for creating sanitation standard operating procedures and thus contribute to reducing the risk of spread of BSE prion via carcasses and meat products contaminated with CNST.

ACKNOWLEDGMENTS. We would like to thank the following people (listed with their organizations at the time) for their cooperation in this study: Ryo Sato (Kenpoku Meat Inspection Office, Tochigi Prefecture); Toru Mabuchi (Meat Inspection Laboratory, Gunma Prefecture); Takayasu Otsuka (Chuo Meat Inspection Center, Saitama Prefecture); Yosuke Kato (Meat Inspection Center, Saitama City); Toshichika Sasaki and Naohito Okazaki (Meat Inspection Center, Ehime Prefecture); Hitoshi Ikeda (Sueyoshi Meat Inspection Center, Kagoshima Prefecture); Naoko Sawada (Shibaura Meat Sanitary Inspection Station Hachioji Branch, Tokyo Metropolitan Government); and Jungo Okajima, Keiko Nakajima, Kazuhiko Shibata and Eiichi Takahashi (Shibaura Meat Sanitary Inspection Station, Tokyo Metropolitan Government). This work was supported by a grant from the Ministry of Health, Labour and Welfare of Japan (17270701).

REFERENCES

1. Anil, M. H., Love, S., Helps, C. R. and Harbour, D. A. 2002. Potential for carcass contamination with brain tissue following stunning and slaughter in cattle and sheep. *Food Control* **13**: 431–436.
2. European Commission. 2002. Update of the opinion on TSE infectivity distribution in ruminant tissue. Available: http://ec.europa.eu/food/fs/sc/ssc/out296_en.pdf
3. EFSA. 2004. Report of the EFSA working group on BSE risk

from dissemination of brain particles in blood and carcass. *EFSA J.* **123** Available: http://www.efsa.europa.eu/EFSA/efsa_locale-1178620753812_1178620777397.htm

4. Helps, C. R., Hindell, P., Hillman, T. J., Fisher, A. V., Anil, H., Knight, A. C., Whyte, R. T., O'Niell, D. H., Knowles, T. G. and Harbour, D. A. 2002. Contamination of beef carcasses by spinal cord tissue during splitting. *Food Control* **13**: 417–423.
5. Iwata, N., Sato, Y., Higuchi, Y., Nohtomi, K., Nagata, N., Hasegawa, H., Tobiume, M., Nakamura, Y., Hagiwara, K., Furuoka, H., Horiuchi, M., Yamakawa, Y. and Sata, T. 2006. Distribution of PrP(Sc) in cattle with bovine spongiform encephalopathy slaughtered at abattoirs in Japan. *Jpn. J. Infect. Dis.* **59**: 100–107.
6. Lim, D. G., Erwanto, Y. and Lee, M. 2007. Comparison of stunning methods in the dissemination of central nervous system tissue on the beef carcass surface. *Meat. Sci.* **75**: 622–627.
7. Masujin, K., Matthews, D., Wells, G. A., Mohri, S. and Yokoyama, T. 2007. Prions in the peripheral nerves of bovine spongiform encephalopathy-affected cattle. *J. Gen. Virol.* **88**: 1850–1858.
8. Prendergast, D. M., Sheridan, J. J., Daly, D. J., McDowell, D. A. and Blair, I. S. 2003. Dissemination of central nervous system tissue from the brain and spinal cord of cattle after captive bolt stunning and carcass splitting. *Meat. Sci.* **65**: 1201–1209.
9. Prendergast, D. M., Sheridan, J. J., Daly, D. J., McDowell, D. A. and Blair, I. S. 2004. Dissemination of central nervous system tissue during slaughter of cattle in three Irish abattoirs. *Vet. Rec.* **154**: 21–24.
10. Ramantanis, S. B. 2006. Alternative cattle slaughtering technologies and/or measures reducing the dissemination of central nervous system tissue during head handling, harvesting of cheek meat and tongue and carcass splitting-a review. *Vet. Arhiv.* **76**: 19–36.
11. Wells, G. A. H., Hawkins, S. A, Green, R. B., Austin, A. R., Dexter, I., Spencer, Y. I., Chaplin, M. J., Stack, M. J. and Dawson, M. 1998. Preliminary observations on the pathogenesis of experimental bovine spongiform encephalopathy (BSE): an update. *Vet. Rec.* **142**: 103–106.
12. Wells, G. A., Spiropoulos, J., Hawkins, S.A. and Ryder, S. J. 2005. Pathogenesis of experimental bovine spongiform encephalopathy: preclinical infectivity in tonsil and observations on the distribution of lingual tonsil in slaughtered cattle. *Vet. Rec.* **156**: 401–407.
13. Will, R. G., Ironside, J. W., Zeidler, M., Cousens, S. N., Estibeiro, K., Alperovitch, A., Poser, S., Pocchiari, M., Hofman, A. and Smith, P. G. 1996. A new variant of Creutzfeldt-Jakob disease in the UK. *Lancet* **347**: 921–925.
14. Yeşilbağ, K. and Kaikan, A. 2005. Detection of central nervous system tissues as BSE specified risk material in meat products in Turkey. *Food Control.* **16**: 11–13.

Available online at www.sciencedirect.com

ScienceDirect

Analytical Biochemistry 370 (2007) 131–141

ANALYTICAL BIOCHEMISTRY

www.elsevier.com/locate/yabio

Detection of prion protein immune complex for bovine spongiform encephalopathy diagnosis using fluorescence correlation spectroscopy and fluorescence cross-correlation spectroscopy

Fumihiko Fujii [a,d], Motohiro Horiuchi [b], Masayoshi Ueno [c], Hiroshi Sakata [a,d], Issei Nagao [a], Mamoru Tamura [a], Masataka Kinjo [a,*]

[a] *Laboratory of Supramolecular Biophysics, Research Institute of Electronic Science, Hokkaido University, Sapporo 060-0818, Japan*
[b] *Laboratory of Prion Diseases, Graduate School of Veterinary Medicine, Hokkaido University, Sapporo 060-0818, Japan*
[c] *Obihiro Research Laboratory, Fujirebio Inc., Kawanishi-cho, Hokkaido 089-1182, Japan*
[d] *Innovation Plaza Hokkaido, Japan Science and Technology Agency, Sapporo 060-0819, Japan*

Received 28 March 2007
Available online 2 August 2007

Abstract

Fluorescence correlation spectroscopy (FCS) and fluorescence cross-correlation spectroscopy (FCCS) are powerful techniques to measure molecular interactions with high sensitivity in homogeneous solution and living cells. In this study, we developed methods for the detection of prion protein (PrP) using FCS and FCCS. A combination of a fluorescent-labeled Fab′ fragment and another anti-PrP monoclonal antibody (mAb) enabled us to detect recombinant bovine PrP (rBoPrP) using FCS because there was a significant difference in the diffusion coefficients between the labeled Fab′ fragment and the trimeric immune complex consisting of rBoPrP, labeled Fab′ fragment, and another anti-PrP mAb. On the other hand, FCCS detected rBoPrP using two mAbs labeled with different fluorescence dyes. The detection limit for PrP in FCCS was approximately threefold higher than that in FCS. The sensitivity of FCCS in detection of abnormal isoform of PrP (PrP^{Sc}) was comparable to that of enzyme-linked immunosorbent assay (ELISA). Because FCS and FCCS detect the PrP immune complex in homogeneous solution of only microliter samples with a single mixing step and without any washing steps, these features of measurement may facilitate automating bovine spongiform encephalopathy diagnosis.

Keywords: Fluorescence spectroscopy; Fluctuation; Diagnosis; Prion protein; Trimeric immune complex; BSE

Transmissible spongiform encephalopathies (TSEs)[1], so-called prion diseases, are fatal neurodegenerative diseases associated with unconventional proteinaceous agents [1]. They include scrapie in sheep and goats as well as bovine spongiform encephalopathy (BSE). A line of evidences suggests that BSE has been transmitted to humans; this disease is designated a new variant of Creutzfelt–Jakob disease (vCJD) [2]. Secondary transmission of vCJD by blood transfusion raised a public concern about the safety of blood transfusion and blood-derived products [3,4]. Therefore, the development of a method for early and sensitive diagnosis is essential to prevent the further spread of prion diseases.

Detection of abnormal isoform of prion protein (PrP^{Sc}) is commonly used for the conclusive diagnosis of prion diseases. At least three different approaches can be used to

* Corresponding author. Fax: +81 11 706 9006.
E-mail address: kinjo@imd.es.hokudai.ac.jp (M. Kinjo).

[1] *Abbreviations used:* TSE, transmissible spongiform encephalopathy; BSE, bovine spongiform encephalopathy; vCJD, variant of Creutzfelt–Jakob disease; PrP^{Sc}, abnormal isoform of prion protein; PrP, prion protein; FCS, fluorescence correlation spectroscopy; FCCS, fluorescence cross-correlation spectroscopy; FCF, fluorescence cross-correlation function; mAb, monoclonal antibody; ELISA, enzyme-linked immunosorbent assay; rBoPrP, recombinant bovine prion protein; PBS, phosphate-buffered saline; Fab′72(532), Alexa 532-labeled Fab′72; mAb72(488), Alexa 488-labeled mAb 72; mAb44B1(647), Alexa 647-labeled mAb 44B1; FAF, fluorescence autocorrelation function; OD, optical density; PK, proteinase K; PrA, protein A; IgG, immunoglobulin G; CSF, cerebrospinal fluid; IU, infectious units; FIDA, fluorescence intensity distribution analysis.

0003-2697/$ - see front matter © 2007 Elsevier Inc. All rights reserved.
doi:10.1016/j.ab.2007.07.018

develop a highly sensitive method for prion diseases using immunobiochemicals as follows: (i) amplification of the amount of PrP^{Sc}, (ii) concentration or enrichment of the amount of PrP^{Sc} from a sample, and (iii) an improvement of the sensitivity in prion protein (PrP) detection. Among these approaches, we aimed to develop a sensitive detection method for PrP.

Analysis of body fluids or tissue extracts ideally should combine minimal sample consumption with high sensitivity. Confocal fluorescence methods are one of the few methods that can do it because they are based on the detection of laser-induced fluorescence emission of dye-tagged single molecules in a very tiny focal volume element of less than 1 fl. Among confocal fluorescence methods, fluorescence correlation spectroscopy (FCS) is a state-of-the-art method based on fluctuation analysis of fluorescence intensity in the confocal volume. The concept of FCS was introduced during the early 1970s [5], and its feasibility in life science was confirmed during the 1990s [6,7]. Because the diffusion time of a small fluorescent molecule through the small detection volume increases on its binding to much larger molecules, measuring the change of its diffusion time by FCS allows detection of antigen using fluorescent-labeled antibody. During recent years, FCS has been applied to investigate biophysical and biochemical processes *in vitro*, such as interaction of chaperon with substrates [8–11], and to analyze microenvironments of living cells and molecular interaction on cell membranes [12–14].

Fluorescence cross-correlation spectroscopy (FCCS) is based on the same principle as FCS, but correlations of two independent signals are determined instead of correlating the fluctuations of one signal. If molecules labeled with two different fluorescent dyes are interacting, only double-labeled compounds contribute to the results of fluorescence cross-correlation function (FCF). Therefore, FCCS enable us to detect antigen using two monoclonal antibodies (mAbs) labeled with different fluorescent dyes [15]. The modern FCCS technique was proposed by Eigen and Rigler during the early 1990s [16] and first realized by Schwille and coworkers [17]. Recently, FCCS has been used to detect the interaction between two molecular species *in vitro* [18–20], and there are reports of *ex vivo* studies [21–23].

Because FCS and FCCS allow characterization of fluorophores in homogeneous solutions without any physical separation steps like those required in other biochemical methods [24], these methods are suitable for high-throughput screening with high sensitivity. In this study, therefore, we employed these techniques to develop the diagnosis methods for prion diseases by detecting PrP. First, we established the method for PrP detection by FCS and FCCS using recombinant PrP as a model. Next, we applied these methods to detect PrP^{Sc} from brain materials of prion-infected animals and compared the sensitivity of FCCS with that of the enzyme-linked immunosorbent assay (ELISA) test approved by the European Commission for BSE diagnosis.

Materials and methods

Recombinant bovine PrP and sample preparation from BSE-negative cattle brains and prion-infected mice brain

Recombinant bovine PrP (rBoPrP) was obtained from Fujirebio (Japan). Medulla oblongata of BSE-negative cattle and brains of mice infected with scrapie Obihiro strain [25] were processed according to the procedure of the FRELISA BSE kit (Fujirebio). After centrifugation at 15,000*g* for 10 min at 25 °C, the pellets were dissolved with 50 μl of urea solution (8 M) and boiled for 5 min. Then the following modifications to the procedure of the kit were made. The solution was centrifuged at 3000*g* for 3 min to remove scattering debris. The supernatant was diluted two- and sixfold with phosphate-buffered saline (PBS, pH 7.3) for ELISA and FCCS analyses, respectively. The concentration of PrP^{Sc} for FCCS analysis, therefore, was 2.3 times less than that for ELISA analysis (350 vs. 150 μl).

Fab'72(532), mAb72(488), and mAb44B1(647)

PrP-specific mAbs 72 and 44B1, which bind to independent epitopes, were used in this study [26].

For FCS analysis, Alexa 532-labeled Fab'72 fragment [Fab'72(532)] was prepared from mAb 72 according to the methods of Yoshitake and coworkers [27]. $F(ab')_2$ fragments of mAb 72 prepared by pepsin digestion were further reduced with 2-mercaptoethylamine to yield Fab' fragments. The fragments were coupled to Alexa 532 maleimide (A-10255, Invitrogen, USA), and then unbound fluorophores were separated using Superdex 200 (16/60, Pharmacia, USA) with 10 mM Tris buffer (pH 7.4) containing 0.05% sodium azide. The labeling ratio was 1.1 dye molecules per Fab'.

For FCCS analysis, mAbs 72 and 44B1 were labeled with an Alexa Fluor 488 Monoclonal Antibody Labeling Kit (A-20181, Invitrogen) and an Alexa Fluor 647 Monoclonal Antibody Labeling Kit (A-20186, Invitrogen), respectively. After purification with the provided spin column, unbound fluorophores were further removed using Slide-A-Lyzer MINI Dialysis Units (Pierce, USA) against PBS (pH 7.4). The labeling ratios were 3.5 and 1.3 dye molecules per 72 and 44B1 antibody molecule, respectively.

FCS and FCCS measurements

The urea-treated samples diluted with PBS (pH 7.3) were mixed with anti-PrP antibodies and incubated for 60 min at 25 °C. The mixtures were subjected to FCS and FCCS measurements. The reaction mixtures were kept for measurement in 384-well chambered coverslips (MP0384120, Olympus, Japan) for MF-20 (Olympus) and 8-well chambered coverslips (Nalge Nunc International, USA) for compact FCCS (Hamamatsu Photonics, Japan). To prevent nonspecific adsorption of proteins on the surface of the coverslip, the sample chambers were treated

with a protein blocker (N101, NOF, Japan) and washed with distilled water before the experiments.

FCS and FCCS measurements were carried out with a modified MF-20 that consisted of a CW Ar^+ laser (488 nm), He–Ne laser (543 nm), and He–Ne laser (633 nm); a water immersion objective (U-Apochromat, 40×, 1.15 NA, Olympus); and two avalanche photodiodes (SPCM CD3017, PerkinElmer, USA). The confocal pinhole diameters were adjusted to 40 μm. The emission signal was detected through a bandpass filter (565–595 nm) on autocorrelation mode excitation at 543 nm. The signals in the cross-correlation mode at 488 and 633 nm were split by a dichroic mirror (625 nm beam splitter) and detected at 510 to 560 nm by the green channel for Alexa 488 and at 650 to 690 nm by the red channel for Alexa 647. The sample volume, temperature, and duration time were 50 μl, 25 °C, and 180 s, respectively.

FCCS measurements were also carried out with a commercial prototype setup, the compact FCCS apparatus (Hamamatsu Photonics), which consisted of two LD pumped solid-state lasers (473 and 635 nm), a water immersion objective (U-Apochromat), and two photomultiplier tubes (H8631-40, Hamamatsu Photonics). The confocal pinhole diameters were adjusted to 100 μm. The emission signals were split by a dichroic mirror (570 nm beam splitter) and detected at 495 to 575 nm by the green channel for Alexa 488 and at more than 650 nm by the red channel for Alexa 647. The sample volume, temperature, and duration time were 10 μl, 25 °C, and 30 s, respectively.

FCS and FCCS data analyses

The fluorescence autocorrelation functions (FAFs) of the red and green channels [$G_r(\tau)$ and $G_g(\tau)$, respectively] and FCF [$G_c(\tau)$] are calculated by

$$G_x(\tau) = \frac{\langle \delta I_i(t) \cdot \delta I_j(t+\tau) \rangle}{\langle I_i(t) \rangle \langle I_j(t) \rangle} + 1, \quad (1)$$

where τ denotes the time delay, I_i is the fluorescence intensity of the red channel ($i = r$) or green channel ($i = g$) and $G_r(\tau)$, $G_g(\tau)$, and $G_c(\tau)$ denote the autocorrelation functions of red ($i = j = x = r$), green ($i = j = x = g$), and cross ($i = r$, $j = g$, and $x = c$), respectively.

Acquired $G(\tau)$ values were fitted by a one- or two-component model as

$$G(\tau) = \frac{1}{N}\left[(1-y)\left(1+\frac{\tau}{\tau_{free}}\right)^{-1}\left(1+\frac{\tau}{s^2\tau_{free}}\right)^{-1/2} + y\left(1+\frac{\tau}{\tau_{bound}}\right)^{-1}\left(1+\frac{\tau}{s^2\tau_{bound}}\right)^{-1/2}\right] + 1, \quad (2)$$

where y denotes the bound ratio of labeled antibody to antigen, τ_{free} and τ_{bound} are the diffusion times of the free and bound molecules, respectively, N is the average number of fluorescent particles in the excitation detection volume defined by radius w_0 and length $2z_0$, and s is the structure parameter representing the ratio $s = z_0/w_0$.

The average numbers of red fluorescent particles (N_r), green fluorescent particles (N_g), and particles that have both red and green fluorescence (N_c) can be calculated by

$$N_r = \frac{1}{C_r(0)}, \quad N_g = \frac{1}{C_g(0)} \quad \text{and} \quad N_c = \frac{C_c(0)}{C_r(0) \cdot C_g(0)}, \quad (3)$$

respectively, where $C_r(0)$, $C_g(0)$, and $C_c(0)$ indicate the amplitudes of the functions $C_r = G_r(\tau) - 1$, $C_g = G_g(\tau) - 1$, and $C_c = G_c(\tau) - 1$, respectively. When N_r and N_g are constant, $C_c(0)$ is directly proportional to N_c. For quantitative evaluation of cross-correlations among various samples, $C_c(0)$ is normalized by $C_g(0)$ [relative cross-correlation, $C_c(0)/C_g(0)$] [21].

The cutoff values of the detection limits for FCS and FCCS were determined from the mean of samples without rBoPrP or PrP^{Sc} plus 3 standard deviations.

ELISA

ELISA-based BSE diagnosis kits, the FRELISA BSE and the Platelia BSE, were obtained from Fujirebio and Bio-Rad (USA), respectively. Optical density (OD) was assessed with a microplate reader (GENios, Tecan Group) at wavelengths of 450 to 620 nm. The cutoff values were determined by the definitions of the kits.

Results

rBoPrP detection by FCS

To distinguish the two components in FCS analysis, their diffusion times must differ by a factor of at least 1.6, which corresponds to a molecular weight ratio of 4 ($= 1.6^3$) [28]. We prepared Fab′72(532) (50 kDa) to detect PrP (30 kDa), and another anti-PrP antibody (mAb44B1, 150 kDa) was also used for weighting to rBoPrP–Fab′72(532). The molecular ratio of the trimeric immune complex 44B1–rBoPrP–Fab′72(532) to Fab′72(532) was 4.6, a value sufficiently above the criterion of 4.

The theoretical diffusion times in Fig. 1A were calculated based on the measured diffusion time of Rhodamine 6G at 543 nm on MF-20 and the molecular weight (0.479 kDa) of Rhodamine 6 G. On the other hand, the obtained diffusion times of the three samples—Fab′72(532), rBoPrP–Fab′72(532), and 44B1–rBoPrP–Fab′72(532)—were in good agreement with the theoretical values. There was no significant difference in the diffusion times between Fab′72(532) and rBoPrP–Fab′72(532), whereas the immune complex 44B1–rBoPrP–Fab′72(532) was clearly distinguished from Fab′72(532). Therefore, we used not only Fab′72(532) but also 44B1 for the detection of rBoPrP by FCS.

Fig. 1B shows the normalized FAFs that shifted to the right with the increase in rBoPrP concentration, indicating

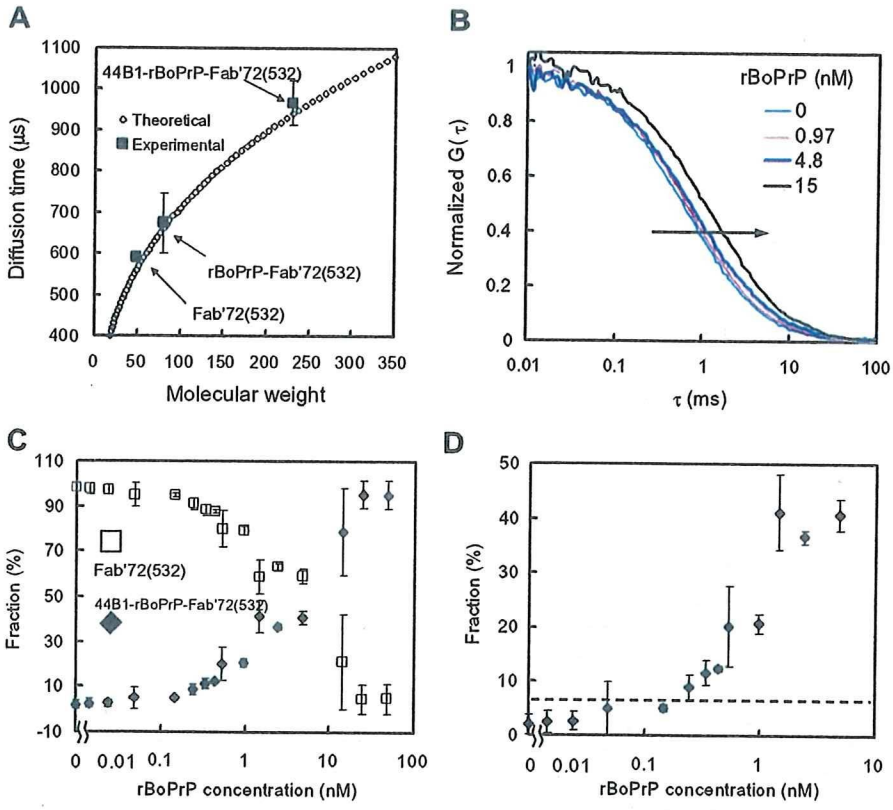

Fig. 1. rBoPrP detection by FCS in PBS (pH 7.3). (A) Theoretical and experimental diffusion times to molecular weight. The experimental diffusion times at the molecular weights of 50, 80, and 230 kDa correspond to Fab'72(532), rBoPrP–Fab'72(532), and 44B1–rBoPrP–Fab'72(532), respectively. (B) Normalized FAFs of Fab'72(532) and the immune complex 44B1–rBoPrP–Fab'72(532). The FAFs were normalized to 1. The arrow indicates the shift of FAF with the increase in rBoPrP concentration. (C) Fractions of Fab'72(532) and the immune complex 44B1–rBoPrP–Fab'72(532). (D) Detection limit for rBoPrP using FCS in PBS (pH 7.3). This is an enlarged graph of panel C. The concentrations of Fab'72(532) and 44B1 used were 0.6 and 50 nM, respectively. The broken line indicates the cutoff value. Data are expressed as means ± standard deviations.

the increasing the fraction of the immune complex 44B1–rBoPrP–Fab'72(532). The diffusion times of FAFs were 670 and 1190 μs at 0 and 15 nM rBoPrP, respectively. We assumed them to be the diffusion times of Fab'72(532) and the immune complex, and then we calculated the fractions (%) of Fab'72(532) and the immune complex in the two-component model of Eq. (2) (Fig. 1C). The fractions of free Fab'72(532) and the immune complex decreased and increased, respectively, with the increase in rBoPrP concentration and reached a plateau at approximately 15 nM. To show the detection limit clearly, we present an enlarged graph of Fig. 1C in Fig. 1D. The value at 0.24 nM rBoPrP remained above the cutoff line when the assay was carried out in PBS (pH 7.3). But the detection limit of FCS was approximately threefold lower than that of ELISA (Bio-Rad) (Table 1).

rBoPrP detection by FCCS in PBS (pH 7.3)

To improve specificity and sensitivity, we further attempted to detect PrP by FCCS using two spectrally independent fluorescent-labeled probes: mAb72(488) and mAb44B1(647). Fig. 2A shows FCFs of the double-labeled immune complex mAb72(488)–rBoPrP–mAb44B1(647). The increase of the amplitude on the y intercept indicates the increasing numbers of the immune complex. For quantitative evaluation of the amplitude, $C_c(0)$ was normalized by $C_g(0)$ in Fig. 2B (see Materials and methods). The value of $C_c(0)/C_g(0)$ at 0.24 nM rBoPrP remained above the cutoff line when the assay was carried out in PBS (pH 7.3). The detection limit of FCCS was comparable to that of ELISA (Bio-Rad) (Table 1).

As shown in Fig. 2C (closed diamonds), unfortunately, the $C_c(0)/C_g(0)$ values of the samples above 14.5 nM rBoPrP were below the cutoff line and assessed as negative. This is because rBoPrP formed the dimeric immune complex with mAb72(488) or mAb44B1(647) instead of the trimeric immune complex mAb72(488)–rBoPrP–mAb44B1(647) at the range of high concentration of rBoPrP. To overcome the limitation, we carried out combination measurements in respective samples, namely, without (closed diamonds) and with (open squares) the addition of 4.8 nM rBoPrP. Fig. 2D shows a criterion for determination as follows. The samples containing no rBoPrP showed negative (−) but showed positive (+) signals by the addition of 4.8 nM rBoPrP. The samples containing 2.42 nM rBoPrP gave

Table 1
Detection limits for rBoPrP and PrP^{Sc} using FCS, FCCS, and ELISAs

Method	rBoPrP		PrP^{Sc} from infected mice (dilution rate)
	in PBS (pH 7.3) (nM)	in BSE-negative samples (nM)	
FCS	0.44 ± 0.13 ($n = 5$)	ND	ND
FCCS	0.13 ± 0.03 ($n = 3$)	0.13 ± 0.03 ($n = 3$)	4^{-6} (0.13 nM)[a] ($n = 3$)
ELISA (Bio-Rad)	0.15 ± 0 ($n = 3$)	0.15 ± 0 ($n = 3$)	ND
ELISA (Fujirebio)	0.05 ± 0 ($n = 3$)	0.11 ± 0.03 ($n = 3$)	4^{-6} (0.30 nM)[b] ($n = 2$) 4^{-7} (0.08 nM)[c] ($n = 1$)

Note. Values are means ± standard deviation of independent experiments. ND, no data.
[a] The value at 4^{-6}-fold was 2.3 times less than that for ELISA because the samples for FCCS were diluted 2.3-fold (350/150 μl) compared with ELISA.
[b,c] The values were determined by the standard curve of the OD value versus rBoPrP concentration in Fig. 4G.

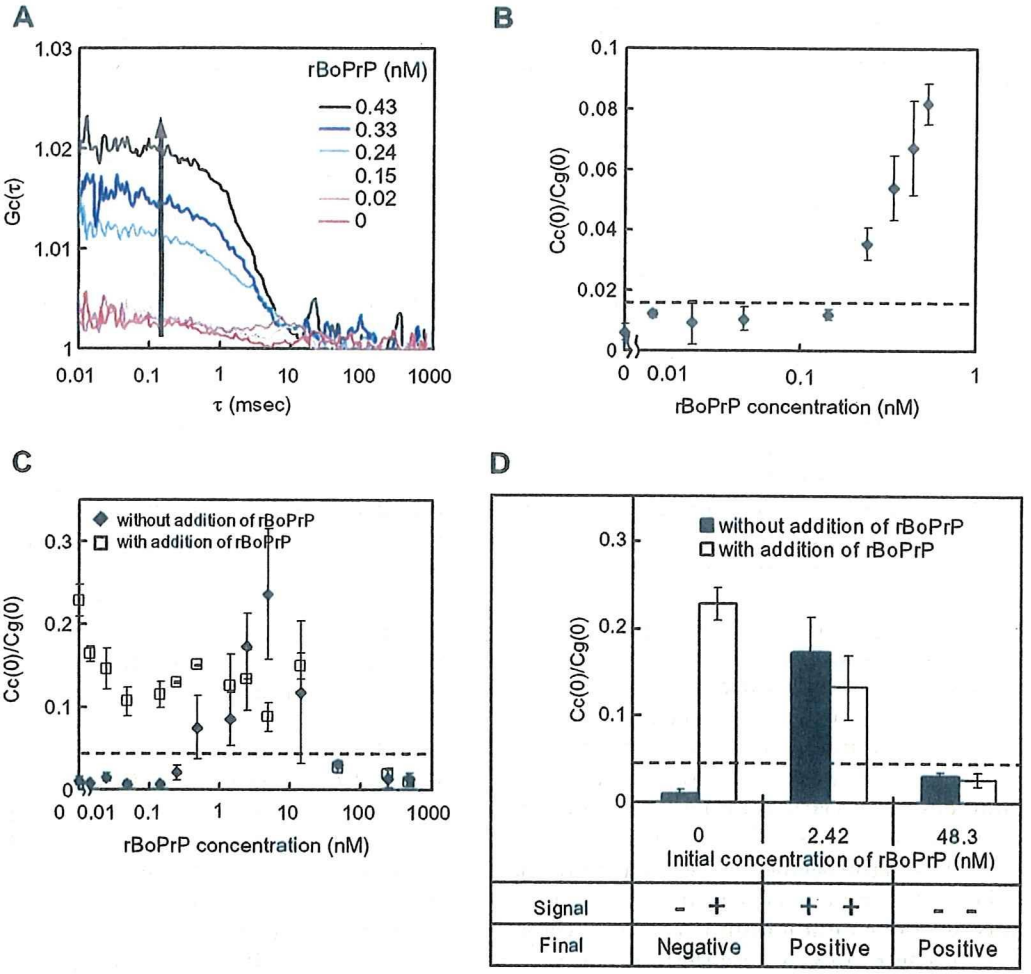

Fig. 2. rBoPrP detection by FCCS in PBS (pH 7.3). (A) FCFs of the immune complex mAb72(488)–rBoPrP–mAb44B1(647). The arrow indicates the elevation of FCF with the increase in rBoPrP concentration. The amplitude on the y intercept of FCF reflects the number of the immune complex. (B) Relative cross-correlation, $C_c(0)/C_g(0)$, with various concentrations of rBoPrP. For quantitative evaluation of cross-correlations, the amplitude of cross-correlation [$C_c(0)$] was normalized by that of autocorrelation [$C_g(0)$]. (C) rBoPrP detection at a broad range of rBoPrP concentration. (D) Criterion for determination. The signals above and below the cutoff line were determined as positives and negatives, respectively. The sample showing negative (−) and positive (+) signals without and with the addition of 4.8 nM rBoPrP, respectively, was assessed as negative. The sample showing negative (+) and positive (+) signals was assessed as positive. The sample showing negative (−) and positive (−) signals was assessed as positive. The concentrations of mAb72(488) and mAb44B1(647) used were 0.1 and 0.1 nM, respectively. The broken lines in panels B, C, and D indicate the cutoff values. Data are expressed as means ± standard deviations.

positive (+) and still gave positive (+) signals by the addition of 4.8 nM rBoPrP. In contrast, the samples containing an excess amount of rBoPrP (48.3 nM) turned negative (−) and still negative (−) even when 4.8 nM rBoPrP was added. By comparison of the two results in each sample, we could make the final decision as to whether the sample was